Contents lists available at GrowingScience

Engineering Solid Mechanics

homepage: www.GrowingScience.com/esm

Structural irregularity: The analysis of two reinforced concrete (r.c.) buildings

Mario Lucio Puppio[a*], Linda Giresini[a], Fabio Doveri[a] and Mauro Sassu[b]

[a]*Department of Energy, Systems, Territory and Constructions Engineering, University of Pisa, Italy*
[b]*Department of Civil, Environmental Engineering and Architecture, University of Cagliari, Italy*

ARTICLE INFO

Article history:
Received 10 October, 2018
Accepted 10 December 2018
Available online
10 December 2018

Keywords:
Multi-storey r.c. buildings
Material variability
Diaphragm flexibility
Irregularity in strength

ABSTRACT

Structural irregularity is a crucial issue in assessing seismic vulnerability of both new and existing buildings. European technical codes provide simple criteria to define irregularities in plan and in elevation, amplifying the seismic actions and/or introducing torsional effects. Nevertheless, this approach only considers geometrical irregularity. For existing buildings, another source of irregularity comes from the non-uniform distribution of the material strength. In particular, for existing reinforced concrete (r.c.) structures, it is possible to detect significant spread of the concrete compressive strength not only from different structural elements but also from different parts of the same member. In this work, non-linear static analysis is performed on two case-studies of r.c. buildings characterized by geometrical and mechanical irregularity. The resistance of each column is determined with an extensive experimental campaign with in situ and laboratory test (about 600 in situ tests). The results are analyzed considering both local and global effects in terms of resistance of the single elements and of the entire buildings. In this sense, shear and bending failure mechanism are taken into account. The effect of storey flexibility is also considered in the models. Fragility curves are calculated for the buildings with random distribution of the compressive strength of the columns. The results are then compared with the approaches proposed by the Eurocodes evaluating in the standard approach proposed by technical codes is conservative or not.

1. Introduction

From the ‘50s, reinforced concrete (r.c.) buildings became more numerous than masonry structures. Nevertheless, most of r.c. buildings in Italy were built without following specific seismic codes, with consequent high vulnerability under earthquake type actions (Bonannini et al. 2017). The seismic response of r.c. building is strictly related to the mechanical behaviour of concrete, depending on its resistance and stiffness. The standard approach of the technical codes (American Society of Civil Engineers (ASCE), 2000; CMIT, 2009; EC8-3, 2005; Manfredi & Masi, 2011) indicates to carry out analysis with the mean values of resistance derived from in situ tests. The dispersion of the strength of material is taken into account only considering a reduction of the design resistance as for example in (FEMA, 2006). In addition, technical codes do not take into account the material variability as source of irregularity. The structural irregularity is only addressed to geometric issues (i.e. geometry and disposition of structural elements, presence of infill walls, etc.).

* Corresponding author.
E-mail addresses: m.puppio@ing.unipi.it (M. L. Puppio)

doi: 10.5267/j.esm.2018.12.002

The seismic capacity of reinforced concrete buildings is usually investigated by means of non-linear static analysis (Bosco et al. 2015a,b c; Fajfar, 2000; Fajfar et al. 2005; Maru & Fajfar, 2005). In literature, several contributions deal with the material variability (Varadharajan et al. 2012) referring to historical constructions made both on masonry and on r.c. buildings. In particular, De Stefano and co-workers analysed the material irregularity considering it both from analytical and numerical point of views (De Stefano et al., 2014; De Stefano & Pintucchi, 2002, 2010; Humar & Kumar, 1999; Lavan & de Stefano, 2013). The analytical approach considers the main variables that affect the problem. The evaluation of the structural response allows to refer to torsionally stiff and torsionally flexible slabs. Torsional effects are also introduced throughout geometrical eccentricity with the aim of taking into account mechanical variability with a simplified method (Bosco et al. 2015 a,b; Mittal & Jain, 1995; Sadek & Tso, 1989). Biondini and co-workers proposed some models that consider aging and decay of the structural materials. In particular are considered the corrosion of the steel bars and the decreasing of the concrete strength due to atmospheric agents (Biondini et al. 2006; 2015; Keskikuru et al. 2001; Titi et al. 2016). The effects of differential decay of concrete and steel on the structural capacity of structural elements are described in (Puppio et al., 2017).

In this paper, the material variability is considered with the aim to evaluate its effects both on local and on global level and to establish whether the traditional approach provided by technical codes is in favour of safety or not. With this purpose, 50 different material distributions are considered for two reinforce concrete buildings, taking into account uniform and varied material distributions. This is done both on local (single structural elements) and on global scale and considering the flexibility of the slabs. The comparison is also made with a deterministic and a probabilistic approach. At a deterministic level is made a comparison for the capacity of single columns in the case of real material distribution with reference to the uniform one.
The current tendency of national codes is oriented towards a probabilistic approach to estimate the seismic capacity of existing buildings (Carley et al., 2004; Consiglio Nazionale delle Ricerche, 2013; Sudret et al., 2014). This requires a great effort in terms of number of analysis. In this case the effects of material variability are considered towards some random material distributions artificially generated from mean value and standard deviation of the real material distribution. All the structural, geometrical and mechanical details of these buildings, part of complex built in the 60s-70s can be found in Sassu et al. (2017).

In Section 2, the effects of concrete variation are examined both in terms of resistance and in terms of stiffness. In Section 3 the two cases of study are presented considering the effective material distribution. The great dispersion in compressive strength of the concrete is shown. In Section 4 the different analyses carried out are considered particularly referred to described material distributions and the results are discussed considering both deterministic and probabilistic approaches, at local and global scale in Section 5.

2. Structural irregularities and strength eccentricities

2.1 Structural irregularity

The results deriving from the analysis of new and existing buildings can be influenced by different irregularities. The current approach in earthquake engineering only considers geometric irregularities (EN 1998-1, 2004). In particular, the irregularities can be defined considering in plan and in elevation issues (EC8-1, 2004; Garcia et al., 2004; Varadharajan et al., 2012). Considering the planimetric distribution is possible to highlight: (1) Symmetry in in-plan configuration - plan configuration shall be compact and, regarding mass and stiffness distribution, approximately symmetric with respect to two orthogonal axes; (2) Shape ratio - the ratio between plan dimensions of a rectangle in which the building plan is inscribed shall be not greater than 4; (3) Presence of set-back or protrusion - No in-plan set-back or protrusion shall exceed 25 % of the building total dimension in the same direction; (4)

Stiffness of slabs - floor slabs can be considered infinitely stiff in their own plan with respect to lateral stiffness of vertical resisting elements and sufficiently strong.

Beyond in plan irregularities it is possible to found vertical irregularities, so categorized: (5) All lateral load resisting systems (such as cores, frames, walls) shall run without interruption from their foundations to the top of the building; (6) Both the lateral stiffness and the mass of individual storeys shall remain constant or vary gradually, without abrupt changes, from the base to the top of the building; (7) For buildings designed with so-called "low ductility", the ratio of storey resistance to the resistance required by the analysis should not vary disproportionately between adjacent floors; (8) When setbacks are present, reductions in the horizontal building section shall occur gradually between adjacent floors. No explicit attention is given to the effects of spatial variation of mechanical properties of the load-bearing elements. Geometrical irregularities are usually introduced in structural analysis increasing the effect towards: (a) The modification of the behaviour factor, a dimensionless parameter to reduce the seismic action); (b) The introduction of the accidental eccentricity that produces torsional effects. (c) The level of knowledge of the real material properties of the structure traduced by means of the confidence factor FC that reduces the strength to be used in the analysis.
Non-linear static analyses are carried out considering the effects of material variability in terms of resistance, maximum displacement and structural ductility. The effects of strength irregularity are evaluated both on local on global scale evaluating whether the standard approach proposed by technical code is in sake of safety or not. In addition, random material distribution are considered in order to obtain fragility curves.

2.2 Material variability and mechanical eccentricity

The seismic response of a r.c. building is strictly related to the mechanical behaviour of the concrete, depending on its resistance and stiffness. The Italian code (EC8-1, 2004) indicates to use for the analyses the average concrete compressive strength f_c from in situ tests, together with the confidence factor (CF) that is associated to the level of knowledge (LK) attained for the structure. Indeed, the design compressive strength is obtained as ratio of the average strength to the confidence factor CF. The higher the level of knowledge, the lower the confidence factor. The LK depends on the number of in situ tests, while the effective distribution of in situ tests and their results do not influence the confidence factor. This can generate some contradictory results, i.e. a confidence factor equal to 1 (CF=1) in case of large number of in situ tests characterized by a wide dispersion of results. FEMA 356 ('Prestandard and Commentary for the Seismic Rehabilitation of Buildings - FEMA 356', 2000) defines the average compressive strength f_c as a function of the coefficient of variation (*cov*) of the data obtained from in situ test (American Society of Civil Engineers (ASCE), 2000). Conventionally, if *cov* > 14%, a proper level of knowledge is not reached and the average compressive strength is reduced by the standard deviation (Eq. (1)).

$$f_c = f_{c,m} - st.dv. \tag{1}$$

Furthermore, if the covariance *cov* < 14% the compressive strength is assumed (Eq. (2)).

$$f_c = f_{c,m}\,. \tag{2}$$

Nevertheless, a relevant dispersion of in situ tests is frequent in existing buildings and in general it is not related to low accuracy in testing. In this sense, it is of interest to evaluate how this physical variation could affect the seismic analysis both in local and global scale. This aspect influences also the stiffness of the building. As well known, further source of irregularity for r.c. constructions are the infill panels. Because of their asymmetrical disposition in the building and because of the shape and the dimensions of the openings, the infill panels can significantly modify the structural response of buildings in terms of stiffness and strength. (Tanganelli et al., 2013).

2.3 Centre of stiffness and centre of resistance

Considering in-plan configuration of a generic building with rigid slabs, the current procedure consists in first identifying the centre of mass (C_M) and centre of stiffness (C_S) as relevant points for the application of seismic forces. In order to take into account irregularity in strength of r.c. columns, it is possible to define the centre of resistance (C_R), as the point conventionally provided by the balance of the strength of each column.

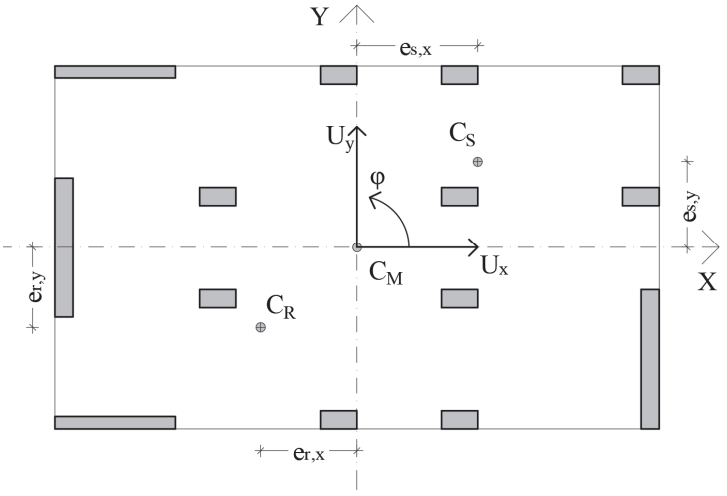

Fig. 1. Main parameters for defining the traditional mechanical eccentricities

The Centre of Stiffness (C_S) is calculated as follows:

$$x_{s,j} = \frac{\sum_{i=1}^{n} x_i K_{y,i}}{\sum_{i=1}^{n} K_{y,i}} \tag{3}$$

$$y_{s,j} = \frac{\sum_{i=1}^{n} y_i K_{x,i}}{\sum_{i=1}^{n} K_{x,i}} \tag{4}$$

where:
x_i , y_i are the coordinates of the centroid of the *i*-th column;
K_{xi} , $K_{yi}$is the stiffness of the *i-th* column (or wall) in one of the main building directions.

The stiffness of a column or of a wall depends on the material elastic modulus. Due to the relation usually adopted for the elastic modulus (CMIT, 2009):

$$E_c = 22'000\left(\frac{f_c}{10}\right)^{0.3} \tag{5}$$

It is straightforward to observe that a variation of concrete compressive strength causes the modification of the centre of stiffness. Then the eccentricity of the centre of stiffness with respect to the centre of masses is:

$$e_{sx,k} = \frac{x_{s,k} - x_{M,k}}{L_{x,k}} \tag{6}$$

$$e_{sy,k} = \frac{y_{s,k} - y_{M,k}}{L_{y,k}} \tag{7}$$

where:
x_M, y_M are the coordinates of the centre of mass;
L_x, L_y are the building dimension in the x and y coordinates.

To define the centre of resistance of the *k*-th floor composed by n columns, it is necessary to establish which of the different mechanisms (axial or shear force, bending moment) has to be considered (Puppio et al., 2017). Regarding the axial forces, the centre of resistance in x and y directions are:

$$x_{R,k} = \frac{\sum_{i=1}^{n} N_{u,i} x_i}{\sum_{i=1}^{n} N_{u,i}}, \tag{8}$$

$$y_{R,k} = \frac{\sum_{i=1}^{n} N_{u,i} y_i}{\sum_{i=1}^{n} N_{u,i}}, \tag{9}$$

where:
$N_{u,i}$ axial strength of the *i*-th columns;
x_i, y_i coordinates of the centre of the *i*-th colums;

Considering now the bending mechanism, it is analogously possible to calculate the centre of resistance through the ultimate bending resistance $M_{ux,i}$ $M_{u,yi}$ of the *i*-th column:.

$$x_{R,k} = \frac{\sum_{i=1}^{n} M_{uy,i}(N_{u,i}) x_i}{\sum_{i=1}^{n} M_{uy,i}(N_{u,i})} \tag{10}$$

$$y_{R,k} = \frac{\sum_{i=1}^{n} M_{ux,i}(N_i) y_i}{\sum_{i=1}^{n} M_{ux,i}(N_i)}. \tag{11}$$

Therefore, the eccentricity of the centre of resistance with respect to the centre of masses is:

$$e_{R,xk} = \frac{x_{R,k} - x_{M,k}}{L_x}, \tag{12}$$

$$e_{R,yk} = \frac{y_{R,k} - y_{M,k}}{L_y}, \tag{13}$$

where:
L_x , L_y are the main dimensions of the buildings in the direction *x* and *y*.

An eccentricity between centre of mass and centre of stiffness (e_S) and between centre of mass and centre of resistance (e_R) generally produces torsional effects in seismic response. In particular, in linear elasticity it is possible to define torsional stiffness of the structure as in Eq. (12) and Eq. (13). The mentioned parameters take into account the main effect of material variability that is the cause of torque component. This leads to a modification of the stresses in elastic and inelastic response as the following analysis shows, in terms of resistance of the bearing elements, ultimate displacements, ultimate shear and ductility.

3. Influence of centre of stiffness on torsional effects (structural response)

In this section, the values of mechanical parameters and their dispersion are accurately evaluated for two cases of r.c. buildings affected by material irregularities by means of experimental in situ tests. From them, the centre of resistance is obtained for each case according to the indications given in Section 2.

3.1. Description of the case study

A vulnerability analysis is carried out on two r.c. school buildings in Italy. Built in the early '70s, is made of four substructures, from A to D (Fig. 2). The three-storey buildings, of a similar in plan total area (about 1000 sqm), are characterized by a high number of slender columns (Fig. 3a). Apparently regular, buildings A and C do not have axes of symmetry because of the position of the stairs and irregularity in elevation, due to greater extension of the ground level. They respectively have a volume of about 10'800 m^3 and an average surface of 990 m^2 at the ground floor and of 615 m^2 at the upper floors.

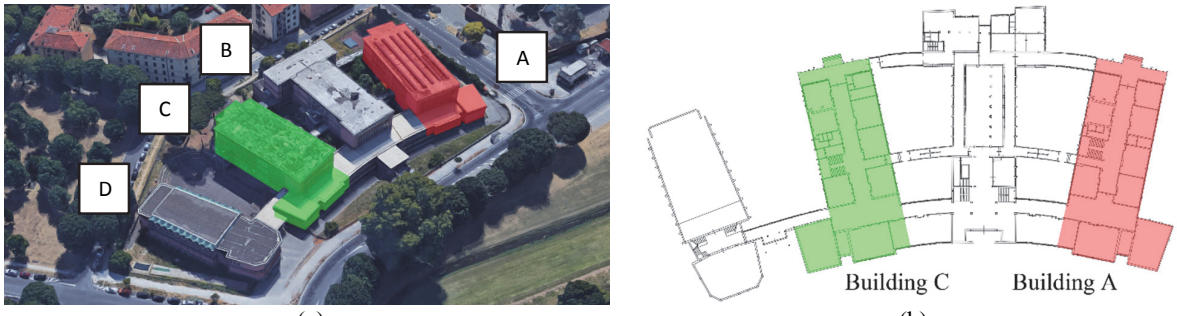

(a) (b)

Fig. 2. Main views of the four buildings. Aerial views (a); identification of the Building A and C (b)

This case study was selected for its significant characteristics in terms of dispersion of mechanical properties and due to its high seismic vulnerability. Such a dispersion is probably to foresee for many other r.c. Italian structures dated back to the sixties and the seventies. The dispersion of concrete compressive strength is mainly due to the lack of standardized procedure of control and automation during the production stage. The concrete was directly produced on site in small batches, so its quality sensitively varied during construction. This aspect is amplified in the case study due to inadequate mix design and procedure of casting and vibration. The large dispersion in concrete compressive strength was noted not only for single structural elements (i.e. beams and columns casted in different time) but also within the same structural member (i.e. at the top and at the bottom of the same column). These structures are generally composed by a series of plane frames. The design approach took into account only vertical and wind loads: this implied weak columns unable to withstand seismic loads and to respect the concept of capacity design. Other elements of weakness, common for r.c. structures of this age, are also un-confined structural nodes and improper anchoring of the bars. In addition, architectural choices were addressed to show the r.c. structures on the facades (Fig.3a), creating further elements of vulnerability as direct exposure to climate events, together with stocky columns (Fig.3b). The main features of the building, in terms of inter-storey height and number of columns, are summarized in Table 1.

Table 1. Main feature of the columns

	Building A		Building C	
Level	h_{int}	n° of columns	h_{int}	n° of columns
0	287	102	300	105
1	408	102	315	105
2	350	98	355	103
3	346	94	351	101
	[cm]		[cm]	

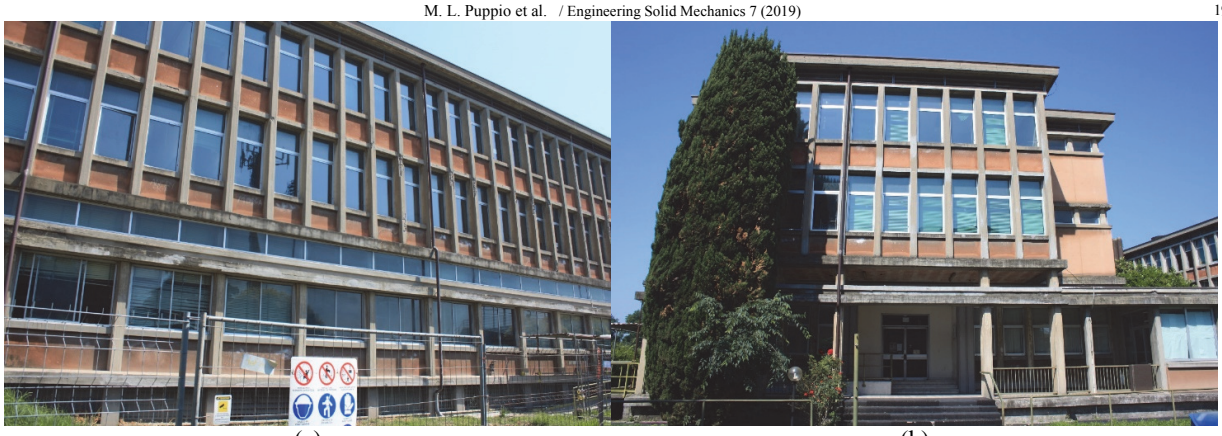

(a) (b)

Fig. 3. External view of the building A. Longitudinal façade (a); Main entrance (b).

3.2. Experimental tests

A large number of tests (Montgomery, n.d.) were made on the structural members of the building A and C of the following type:

1. Tensile strength of reinforcing bars;
2. Compressive strength of coring samples;
3. Schmidt hammer test of the columns.

The results are shown in Table 2. A great dispersion both in concrete and in steel resistance is observed. In this work the variation of steel resistances are neglected. The mean values and the relative standard deviation for building A and C are summarized in Table 5.

Table 2. Experimental test

	Concrete coring	Steel failure test-Steel reinforcing	
N (Number of test)	f_c (Compressive strengh) [MPa]	f_y (Yield steel strength) [MPa]	f_t [MPa]
1	18.7	388	574
2	49.6	506	605
3	25.0	366	529
4	53.2	398	584
5	34.6	373	544
6	32.4	401	537
7	16.2	388	559
8	11.6	356	469
9	17.4	362	473
10	48.1	385	539
11	36.7	375	510
12	28.7	379	512
13	42.3		
14	36.9		
15	30.0		
16	30.0		
17	21.4		
18	46.5		
Average	32.2	389.8	
Standard deviation	12.4	39.1	

The hummer tests are made on 70% of the 294 columns of Building A and on 90% of the 309 columns of the Building C. Experimental tests on Building C are carried out during the phase work of seismic rehabilitation of the structure, obtaining about 600 sclerometeric data as shown in Appendix A.

4. Analysis and numerical models

The models of the Buildings A and C is made by continuous beam frames (Fig. 4). Building A is made by 823 elements and 508 joint nodes (3048 DOF) while Building B is made by 833 elements and 546 nodes (3276 DOF). Both the models are fixed to the ground.

The eccentricity between beams and columns is modelled throughout rigid links. This happens in correspondence of squat beam and columns.

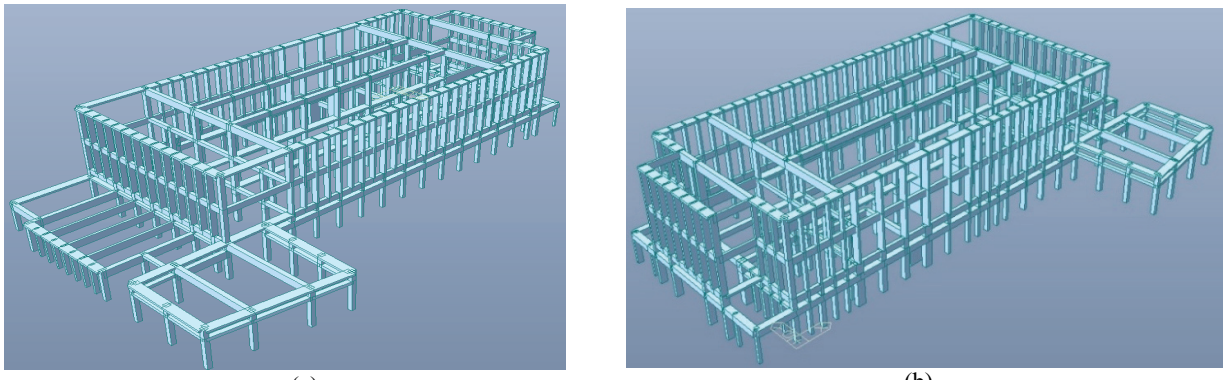

(a) (b)

Fig. 4. Main view of the structural models of the Buildings (a) and (b)

The two buildings are modelled separately by technical joints at the first level of the structure. Two limit scenarios are considered modelling both rigid and flexible slabs. The slabs are modelled with rigid slabs and with flexible diaphragms, by using plate elements (about 500) with proper thickness and stiffness. The flexible diaphragms are noticeable in the evaluation of the effects of material variability as shown in the introduction. The flexibility of the slab has a relevant role (Sassu et al., 2017), modifying the actions on elements characterized by different resistance and stiffness: i.e., in most cases rigid slab can maximise the actions on the bearing elements far from the centre of stiffness. The beams are modelled as elastic frames, neglecting their ductile capacity. The columns are modelled with mechanical non linearities introducing plastic hinges for shear and bending mechanism. A more proper model would consider a discretization of the ends of the columns by means fibres subjected to uniaxial stress (Bosco et al. 2015). The shear failure mechanism is also introduced for squat elements (Puppio et al., 2017), due to their slenderness or by the effect of infill walls or other non-structural elements (Çelebi et al., 2010). Non-linear static analyses are carried out by means of FEM Software Midas Gen v.1.1. The slabs are modelled with rigid slabs and with flexible diaphragms, by using plate elements.

4.1 Material distributions

The goal of the analysis is to evaluate whether the approach of Technical Code (Eurocode and NTC) is conservative or not in seismic vulnerability. With this purpose, several configurations of column strength, with the same mean value, are analysed:

1. Uniform - (Distribution 1), given by technical codes (f_{ca} for all the columns);
2. Actual - (Distribution 2), with the effective compressive strength for each column as measured from experimental tests. Where was not possible to measure f_{ci} the mean value f_{ca} is considered;
3. Extreme - (Distributions 3 - 10), it is assumed the maximum ($f_{c,i}+\Delta f_{ci}$ and $f_{c,i}-\Delta f_{c,i}$) and the minimum strength values as shown in Fig. 5;
4. Random - (Distributions 11 - 60), generating 50 random distributions with same mean value.

Distributions 1 and 2 are used to compare the two structures with the code assumptions and with actual conditions. Distributions 3-11 evaluate the effect of extreme material distribution as shown in Fig. 5, to obtain corresponding resistance domains. The approach used here considers only the spatial variability of strength distribution and neglects possible effect in non-symmetric introduction of the seismic input (Andreini et al., 2014). The random distributions (Case 4) are used to obtain fragility curves related to different limit states.

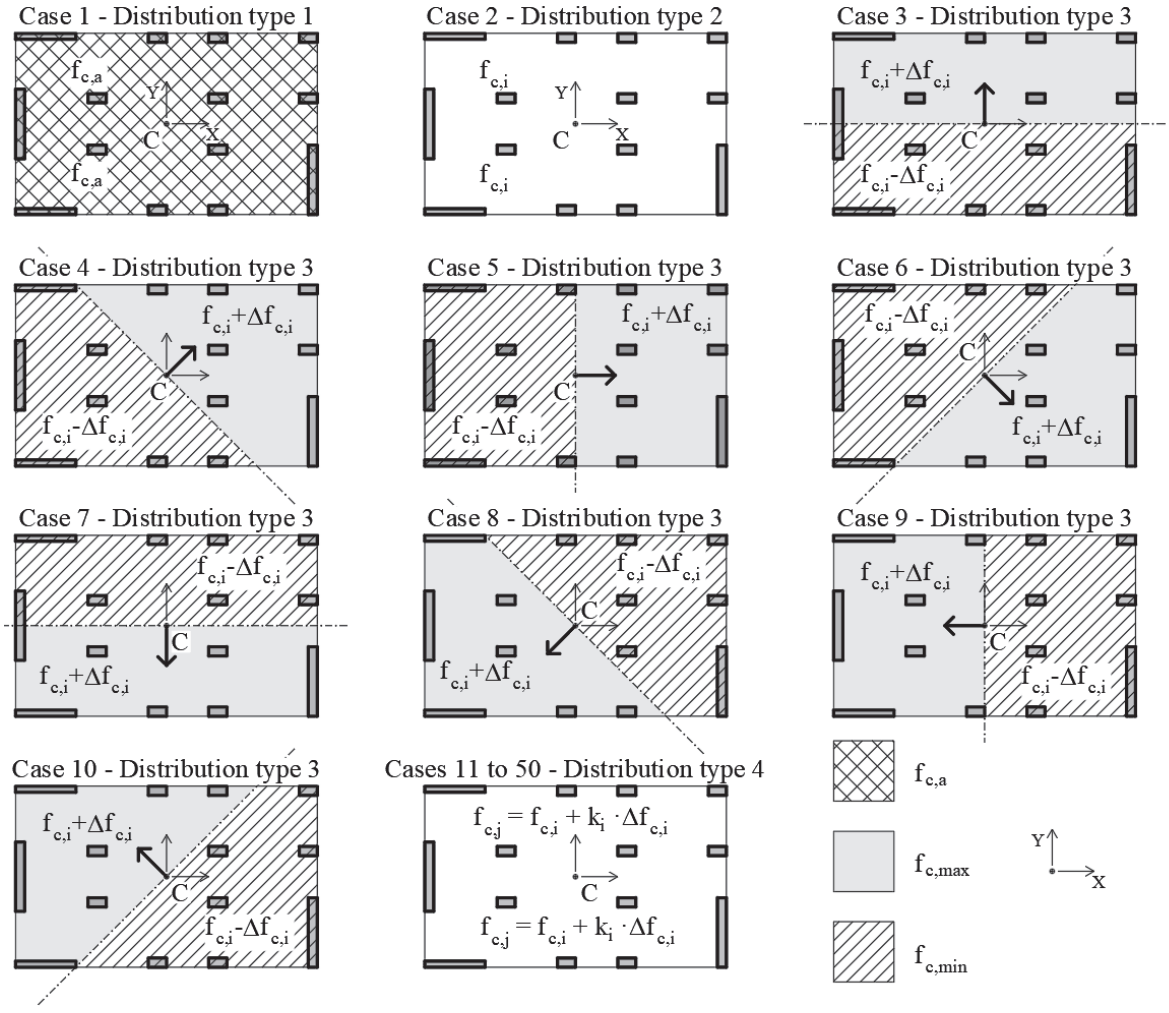

Fig. 5. Material distribution cases

The procedure used to generate fragility curves is:

1. Generation of the random vectors (k_j). - The superscript *j* is the number of the vectors and consequently of the structural analysis; the vectors k_j have average value equal to zero and standard deviation equal to one;
2. Determination of the cylindric compressive strength for the *i*-th column. This is generated according to:

$$f_{c,i} = f_{c,avg} + k_{i,j} \cdot \Delta f_c \tag{14}$$

in which $k_{i,j}$ is the *i*-th component of the *j*-th vector. This ensures that each random distribution *j* has the same average value ($f_{c,avg}$) and the same standard deviation (Δf_c) as the uniform one.

3. Determination of the elastic modulus for the *j*-th columns:

$$E_{c,i} = 22.000\left(\frac{f_{c,i}}{10}\right)^{0.3} \tag{15}$$

4. Non-linear static analyses are carried out for each distribution of ($f_{c,i}$; $E_{c,i}$);
5. Calculation of the PGA related to the considered limit states;
6. Determination of the fragility curves.

The data used here follow a Log-Normal distribution. For this reason, the probability of reaching the analysed limit state is calculated with:

$$P_f = \Phi\left[\frac{\log\left(PGA_i\right) - \log\left(PGA_{avg}\right)}{\chi}\right] \tag{16}$$

in which:

PGA_j is the value of PGA related to *j*-th distribution;

PGA_{avg} is the average value of PGA;

Φ is the function that expresses the density distribution;

χ is the Standard Deviation of the logarithm of the population of the PGA_i:

$$\chi = ST.DEV\left(\log\left(PGA_i\right)\right) \tag{17}$$

For each case two different models are considered: model (1) with rigid slabs and (2) with flexible diaphragms. The global effects can be described by the following three dimensionless parameters:

$$\alpha = \frac{V_u^R - V_u^U}{V_u^U} \tag{18}$$

$$\beta = \frac{d_u^R - d_u^U}{d_u^U} \tag{19}$$

$$\gamma = \frac{\mu_d^R - \mu_d^U}{\mu_d^U} \tag{20}$$

in which:

V_u is the ultimate shear (CMIT, 2009; EC8-1, 2004);

d_u is the ultimate displacement of the control-point;

μ_d is the ductility.

while the apices:

R is referred to the Real material distributions (Case 2), and

U is referred to the Uniform material distributions (Case 1).

The parameters α, β and γ are respectively representative to the ultimate shear (V_u), to the ultimate (d_u) displacements and to the ductility (μ_d) of the structures. The obtained data are reported in Table 3.

Considering the average value in Table 3 is possible to obtain α=-5%; β=-8% and γ=-4%. The data in Table 3 are referred to the PO cases here described and the comparison is made both for flexible and rigid slabs. The comparison, made for real and uniform material distribution, highlighted that there is a dispersion in the results both in terms of ductility (γ) and in terms of ultimate displacement (β). In several cases the adoption of the real material distribution produced results more severe with respect to the uniform one. This means that the uniform material distribution is not safe. In fact, from the average values of the analysis is evident a reduction of the 5% of α and of the 8% of β. The more representative P.O. curves are reported in Fig. 6. “T” and “A” are respectively referred to the distribution of forces from modal dynamic analysis and to that proportional to masses (uniform acceleration).

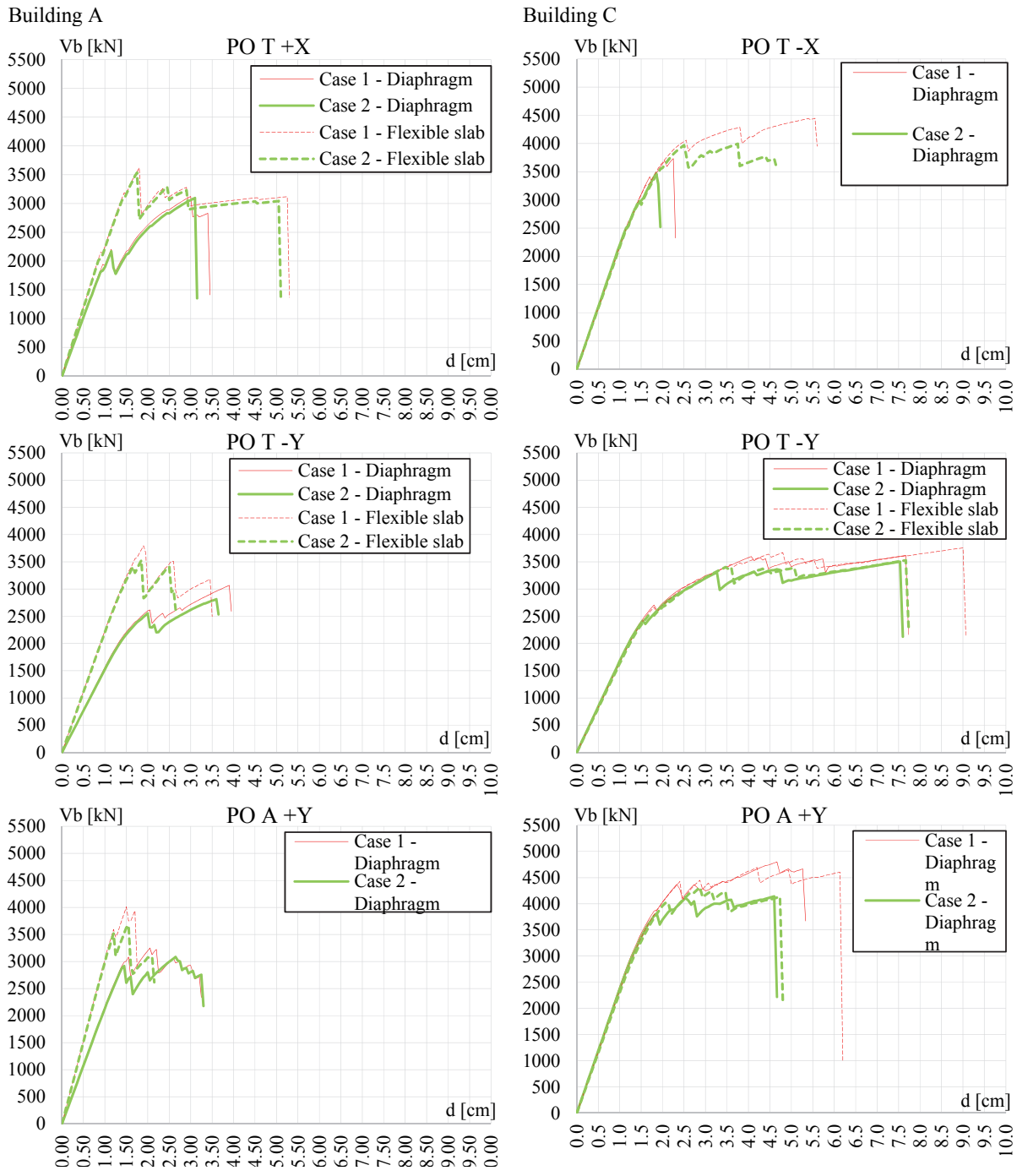

Fig. 6. P.O. curves for Building A and C in case of Uniform and real material (considering rigid and flexible slab)

Actual and uniform material distributions do not show great differences in terms of ultimate shear (due to the same mean value of compressive strength of the two distributions) but exhibit significant differences in terms of ultimate displacements. Furthermore, the diagrams in Fig. 7 highlight that the main differences between capacity curves are due to the stiffness of the slab.

Table 3. Parameter α, β and γ for the Buildings A and C

	Rigid slab						Flexible diaphragm					
	$\alpha_{loc.}$	$\alpha_{aver.}$	$\beta_{loc.}$	$\beta_{aver.}$	$\gamma_{loc.}$	$\gamma_{aver.}$	$\alpha_{loc.}$	$\alpha_{aver.}$	$\beta_{loc.}$	$\beta_{aver.}$	$\gamma_{loc.}$	$\gamma_{aver.}$
Building A	-1%	-1%	-9%	-7%	-13%	-8%	-2%	-6%	-4%	2%	-1%	11%
	-3%		-4%		-9%		-10%		-9%		-8%	
	5%		-11%		-13%		-2%		-4%		6%	
	-8%		-8%		-5%		-7%		-24%		-25%	
	0%		-4%		-2%		-4%		26%		39%	
	-5%		2%		-15%		-8%		22%		30%	
	7%		-20%		-10%		-6%		-8%		18%	
	-7%		-6%		2%		-6%		17%		25%	
	$\alpha_{loc.}$	$\alpha_{aver.}$	$\beta_{loc.}$	$\beta_{aver.}$	$\gamma_{loc.}$	$\gamma_{aver.}$	$\alpha_{loc.}$	$\alpha_{aver.}$	$\beta_{loc.}$	$\beta_{aver.}$	$\gamma_{loc.}$	$\gamma_{aver.}$
MoBuilding C	-6%	-7%	-18%	-12%	-14%	-6%	-6%	-6%	-27%	-16%	-24%	-11%
	-12%		-1%		6%		-9%		-7%		5%	
	-7%		-15%		-6%		-10%		-17%		-12%	
	-3%		-2%		2%		-6%		-14%		-9%	
	-3%		-20%		-18%		-2%		-20%		-23%	
	-14%		-14%		0%		-8%		-23%		-17%	
	-9%		-25%		-17%		-5%		-9%		2%	
	-6%		2%		-3%		-5%		-15%		-13%	

4.1.1 Local effects

The effects of material variability are also evaluated for single structural members. In particular, brittle mechanisms are verified in terms of resistance whereas ductile mechanism is verified in terms of displacement-capacity. The effects of the variation in concrete compressive strength are illustrated in (Puppio et al., 2017). Resistance (or demand D) and capacity C verification can be expressed as their ratio R:

$$R = \frac{D}{C} \tag{21}$$

In particular, in Fig. 7 in case of actual concrete compressive strength (R) is compared with the conventional case of Uniform compressive strength distribution (U):

$$\Delta = \left(\frac{D}{C}\right)_R - \left(\frac{D}{C}\right)_U \tag{22}$$

Eq. (22) furnishes a comparison of the local effects on a generic bearing element. In particular Δ is a number greater than zero if the uniform material distribution (Case1) produces an unsafe condition and it is a number smaller than zero if produces a safe condition. Fig. 7 and Fig. 8 show the results in terms of Δ compared for the ground floor of the building A and C. For the sake of brevity only the elements with Δ > 10% are shown in Table 4 (unsafe condition). In Figs. 7-8, the percentages in blue are referred to ductile mechanisms, while the ones in red are referred to the brittle mechanisms. For each layout the number of elements for which the capacity is underestimated is reported (Table 4).

Table 4. Percentage of Elements with Under-estimated Capacity (P.E.U.C.) for different failure mechanism.

	Pushover direction	Failure mechanism	Δ_{max}	Δ_{ave}	Δ_{min}	P.E.U.C.
Building A	X	My	10%	21%	52%	21%
	X	Fz	10%	20%	50%	15%
	Y	Mz	17%	67%	89%	29%
	Y	Fy	12%	66%	98%	29%
Building C	X	My	13%	50%	100%	10%
	X	Fz	10%	26%	73%	16%
	Y	Mz	10%	48%	96%	6%
	Y	Fy	10%	31%	98%	11%

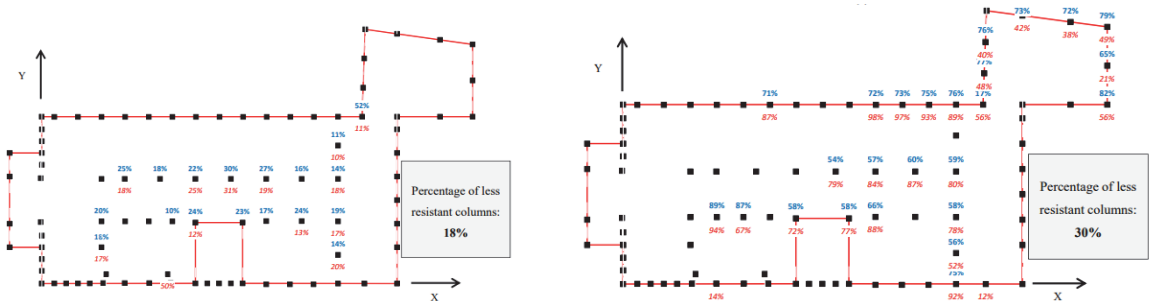

(a) (b)

Fig. 7. - Local effects of P.O. analysis. Delta values for the ground floor of Building A. In blue bending mechanism and in red brittle mechanism. Push over in X dir. (a) and in Y dir. (b)

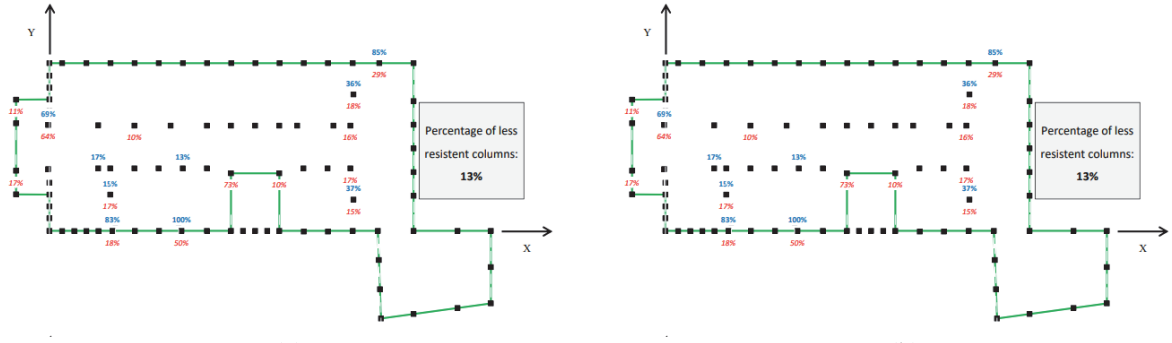

(a) (b)

Fig. 8. Local effects of P.O. analysis. Delta values for the ground floor of Building C. In blue bending mechanism and in red brittle mechanism. Push over in X dir. (a) and in Y dir. (b)

4.2. Fragility curves from random distribution

In order to obtain a probabilistic evaluation of the seismic vulnerability, further analyses are carried out with random distributions of concrete strength of the columns. Fifty random distributions are performed for each building with the same mean value and the same standard deviation of the real case (Shinozuka et al. 2000). These values are indicated in Table 5

Table 5. Main data for concrete for Building A and C

		Building A	Building C
		f_c	f_c
Average value	[MPa]	35.6	30.5
Standard deviation	[MPa]	13.5	12.1
CV	[%]	38%	40%

The limit states are defined with the method proposed by Vona (2014) and the indications of EMS-98 (Grünthal, 1998) summarized in Table 6.

Table 6. Limit states for structural damages in non-linear static analysis - EMS 98 (Grünthal, 1998)

Limit state	Structural Damage	Repairability	Interstory Drift
LS0	No damage	-	$d_r < 0.0010 \cdot h$
LS1	Weak – No structural damage	Total	$0.0010 \cdot h < d_r < 0.0025 \cdot h$
LS2	Moderate – limitated structural damage	Easily repairable	$0.0025 \cdot h < d_r < 0.050 \cdot h$
LS3	Significant – extensive structural damage	High restoring cost	$0.0050 \cdot h < d_r < 0.0100 \cdot h$
LS4 – LS5	High – Structural Collapse	Difficult to repair	$0.0100 \cdot h < d_r$

The procedure to determine fragility curves is described in Section 0. The main parameters to generate them are summarized in Table A1.

Table 7. Main value

	Building A - Dir. X		Min	Max	Average	Standard Dev.
ULS	Normal	[%g]	0.042	0.071	0.061	0.007
	Log-Normal	[-]	-3.170	-2.645	-2.806	0.119
DLS	Normal	[%g]	0.029	0.065	0.045	0.007
	Log-Normal	[-]	-3.540	-2.733	-3.109	0.168

	Building A - Dir. Y		Min	Max	Average	Standard Dev.
ULS	Normal	[%g]	0.044	0.070	0.059	0.007
	Log-Normal	[-]	-3.124	-2.659	-2.845	0.118
DLS	Normal	[%g]	0.029	0.063	0.043	0.008
	Log-Normal	[-]	-3.540	-2.765	-3.152	0.175

	Building C - Dir. X		Min	Max	Average	Standard Dev.
ULS	Normal	[%g]	0.049	0.088	0.060	0.007
	Log-Normal	[-]	-3.016	-2.430	-2.816	0.123
DLS	Normal	[%g]	0.029	0.072	0.044	0.007
	Log-Normal	[-]	-3.540	-2.631	-3.131	0.177

	Building C - Dir. Y		Min	Max	Average	Standard Dev.
ULS	Normal	[%g]	0.044	0.082	0.063	0.008
	Log-Normal	[-]	-3.124	-2.501	-2.768	0.123
DLS	Normal	[%g]	0.029	0.068	0.047	0.008
	Log-Normal	[-]	-3.540	-2.688	-3.082	0.177

In Fig. 9 the fragility curves related to buildings A and C are displayed. The fragility curves are both for damage limit state (DLS) and for ultimate limit state (ULS). With a dashed vertical line are also shown the values of PGA_d related to the Operating Limit State and to Damages Limit State related to the building site.

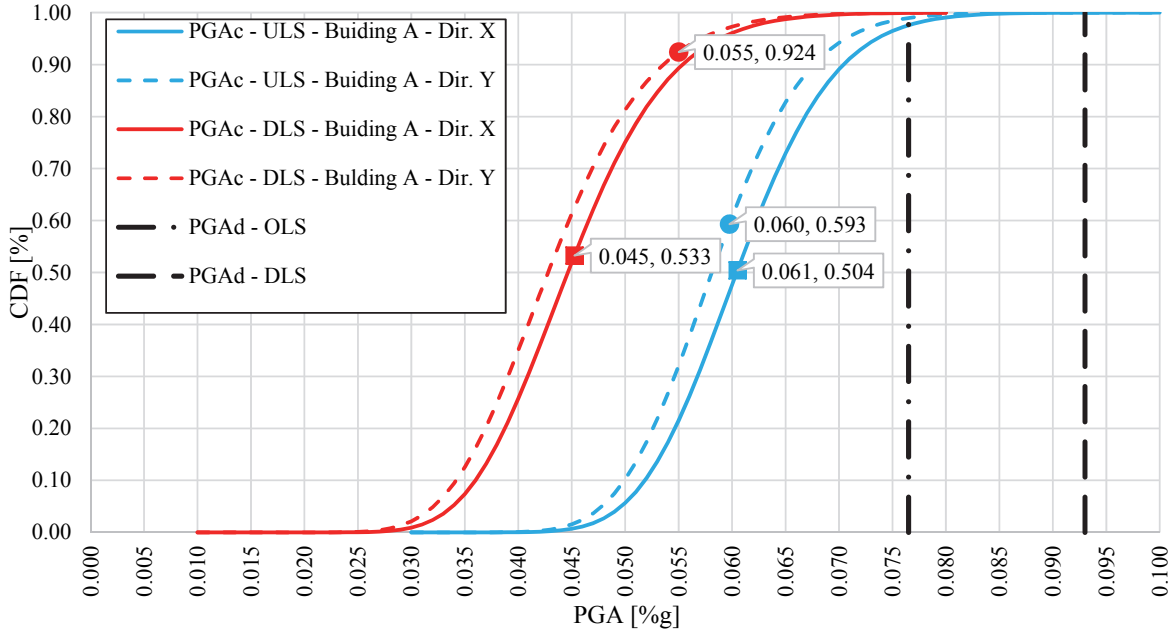

Fig. 9. Fragility curves for DLS and ULS for building A. The Square and the circle in the graph represent the value of PGA related to the uniform material distribution (Case 1). The numbers into the rectangles complete are ...

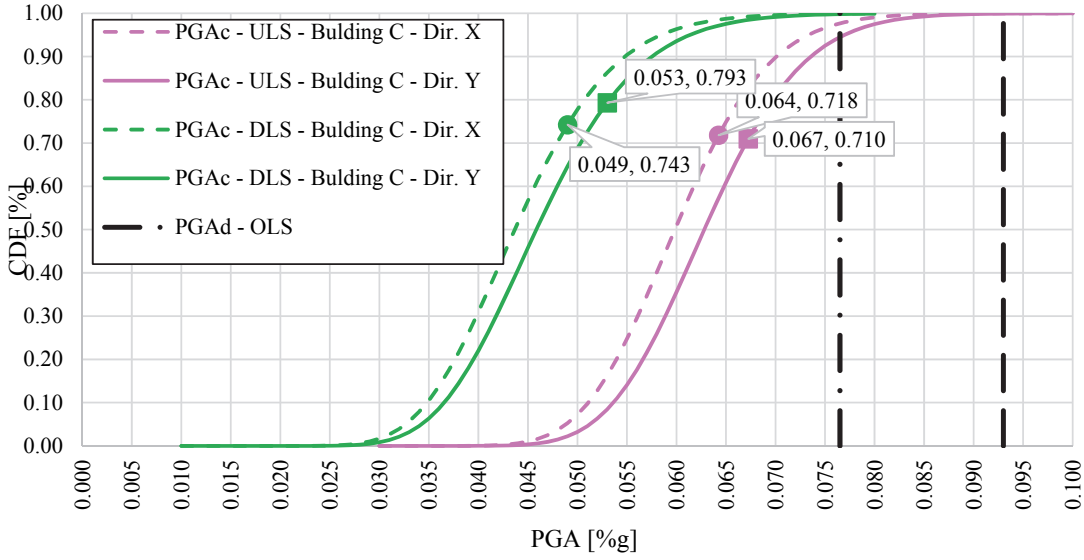

Fig. 10. Fragility curves for DLS and ULS for building C. The square and the circle in the graph represent the value of PGA related to the uniform material distribution (Case 1). The numbers into the rectangles indicat ....

In addition, Risk Indexes are calculated with the following three different formulations, by means shear force, PGA and return period T_r.

$$IR_{Vb} = \frac{V_{b,C}}{V_{b,D}} \tag{23}$$

$$IR_{PGA} = \frac{PGA_C}{PGA_D} \tag{24}$$

$$IR_{T_r} = \left(\frac{T_{R,C}}{T_{R,D}}\right)^{0.41} \tag{25}$$

where:
PGA is the peak ground acceleration;
Tr is the return period.
while in Eq. 23-25 the subscript C is the capacity and D is the demand;

The risk indexes assume values lower than 1 in all the analyses, i.e. the structure has not the proper capacity to withstand seismic actions. The histograms in Fig. 11 and Fig. 12 represent the risk indexes of the structure evaluated with Equations 23-25 relative to the cases from 1 to 10 (Fig. 5). The extreme material distribution shows the main difference with respect to the uniform one (1). The real material distribution (2) present risk indexes, indicative of global effects, that are nearest to the uniform one (1).

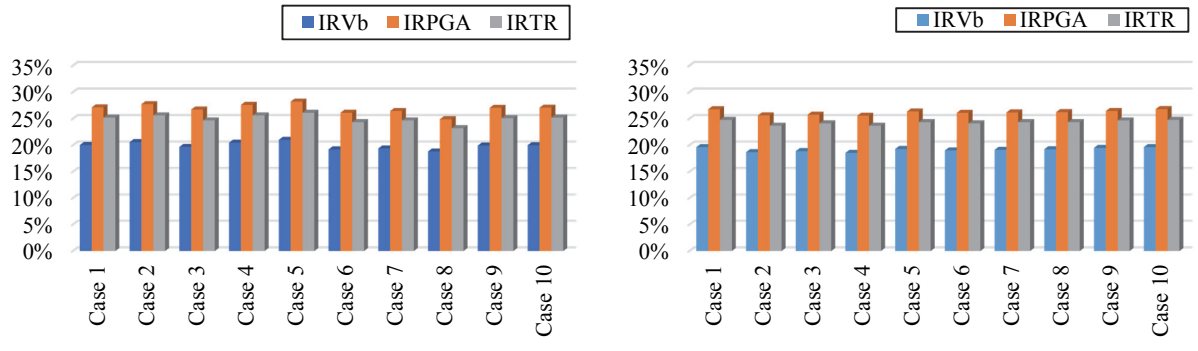

Fig. 11. Risk indexes for Building A in X dir. (a) and in Y dir. (b). Eq. (23)-(25).

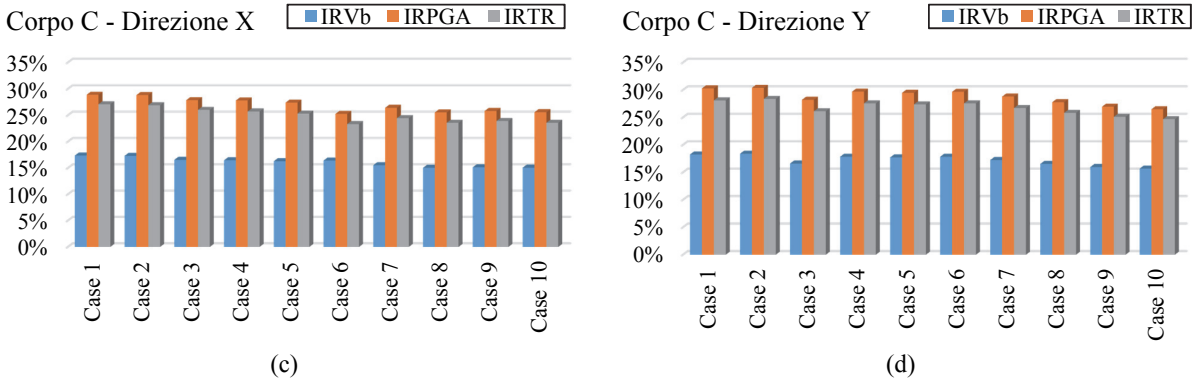

Fig. 12. Risk indexes for Building C in X dir. (c) and in Y dir. (d). Eq. (23)-(25).

5. Discussion of results

The comparison between different models is made in terms of local and local verification.

5.1. Local verification

Regarding the local verification of the single structural elements it was verified that to consider the real material distribution (Case 2) is not in sake of safety. In this case the capacity is over-estimated for about a maximum of the 31.0% of the numbers of the structural elements with respect to the uniform material distributions (Case 1). This comparison is made only for the models with rigid slab. Taking into account the effective resistance of the bearing elements produces effects both on ductile and on brittle failure mechanisms as shown in (Puppio et al., 2017). The effects of the real material distributions are shown in Table 8.

Table 8. Percentage of elements with underestimated capacity.

	Building A		Building C	
	Ductile	Brittle	Ductile	Brittle
POT +X	20.7%	14.9%	10.0%	15.6%
POT+Y	28.7%	31.0%	5.6%	11.1%

5.2. Global verification

Considering the global analysis of the structures the comparison can be made in terms of: (1) defined parameters (α, β, γ) (Eqs. (18-20)); (2) risk indexes; (3) fragility curves. As for (1), the hypothesis of flexible slabs makes extreme the value of the parameters (Eqs. (18-20)). Considering the average values for α, β, γ one has some variation always lower than zero. This means that considering the effective resistance of the structural elements produces a reduction of the performances of structural elements in terms of global shear, in terms of displacements and, consequently, in terms of ductility. Therefore this approach that is of course more realistic should be recommended in the seismic analysis.

5.3. Risk indexes

Risk indexes vary in the range from 15% to 30% according to whether they are calculated in function of the global shear (IR_{Vb}), of the peak ground acceleration (IR_{PGA}) or of the relative return period (IR_{Tr}). Considering the real strength distribution usually does not lead to a decrease of the global safety. The extreme material distributions lead to a major difference highlighting that some distribution of materials can affects the vulnerability of the buildings. In particular the extreme material distributions (Cases from 3 to 10 in Fig. 5) have values less than the 3.0% if referred to the uniform one. This difference is very small in absolute terms (about 10% in relative terms). Considering the

small variation of the risk indexes towards the reference distribution (Case 1) the extreme material distribution can be considered as lines of level of the function risk index (Puppio et al., 2017).

5.4. Fragility curves

The fragility curves express the cumulate distribution of the PGA values for ULS and DLS. These are obtained for both the buildings considering some random strength distributions (Case from 11 to 50 in Fig. 5). In Fig. 9 the fragility curves related to building A are displayed. The square and the circle represent the point - Case 1. Although the random material distributions are determined with the same means of the uniform one, the points representing the latter are placed beyond the half of the fragility curves. This means that most of the analysed random cases presents PGA of collapse that is lower than the PGA related to Case1.

$$PGA_{3...10} < PGA_1 \tag{26}$$

Is it also possible to observe that, also considering a probabilistic approach, the uniform material distribution is not in sake of safety.

5.5. Comparison with conventional approaches

In the current structural modelling of the structure Technical Codes consider the elastic and the inelastic approach as alternative methods. The action derived from elastic approach produced a more severe design of the structural elements. In case of inelastic analysis, it is possible to adopt all the actions that act indifferently on structural elements. This approach reduces the concentration of the actions producing a less expensive design. It is possible to consider these two approaches referring to the centre of stiffness and to the centre of resistance of the structure. In particular: (1) in linear elastic analysis the material variability is taken into account considering a variation in the position of the centre of stiffness and the more severe effects of slab torsions; (2) in non-linear analysis it is possible to considers the variation in the positions between centre of mass and centre of stiffness evaluating the effects on the results.

6. Conclusions

The introduction of the material variability produces changes in structural response both in local and global terms. The evaluation of the structural response of existing buildings has therefore to consider the variability of the material strength. This can be done when, considering a limited number of experimental tests, it is possible to find a relevant dispersion of the strength values. In r.c. buildings, the dispersion of concrete compressive strength can affect the structural response and the verification of the elements. In particular the variation of compressive strength can have some effects both in ductility and in the failure mechanism. In order to obtain some simplified methods to take it into account it should be recommended to:

- introduce some extreme distributions of resistance referred to the minimum and the maximum values (cases 3-10);
- evaluate how to the considered building is prone to torsional effects (particularly for linear elastic analysis).

These methods are highlighted in the paper referring to two cases of study. Non-linear static analyses are carried out considering rigid and flexible slabs. In general, the results show that the flexible slab produces more significant variation in structural response.
In the verification of local elements it was highlighted that for some elements, to take into account the effective resistance of the material produces an effect that is not in sake of safety in structural

verification. The global indicator of the structural response (index of risk) exhibits a reduced variation from the comparison between Case 1 and Case 2. The information related to how the material variability affects the structural response is also useful to better evaluate a possible strategy of intervention. Interventions that allow the reduced the material eccentricity thanks to the construction of a new bracing system have to be preferred.

Acknowledgment

The Authors would like to sincerely thank the Province of Lucca for technical data on material provided and used for the analyses.

References

Alecci, V., Briccoli Bati, S., & Ranocchiai, G. (2009). Study of Brick Masonry Columns Confined with CFRP Composite. *Journal of Composites for Construction* , *13*, 179–187.

American Society of Civil Engineers (ASCE). (2000). FEMA 356 Prestandard and Commentary for the Seismic Rehabilitation of Building.

Andreini, M., Caliò, I., Cannizzaro, F., De Falco, A., Giresini, L., Pantò, B., & Sassu, M. (2014). Seismic assessment of the historical mixed masonry-reinforced concrete government Palace in La Spezia. In *9th International Conference on Structural Analysis of Historical Constructions*.

Biondini, F., Bontempi, F., Frangopol, D. M., & Malerba, P. G. (2006). Probabilistic service life assessment and maintenance planning of concrete structures. *JOURNAL OF STRUCTURAL ENGINEERING-ASCE*, *132*(5), 810–825.

Biondini, F., Camnasio, E., & Titi, A. (2015). Seismic resilience of concrete structures under corrosion. *Earthquake Engineering and Structural Dynamics*, *44*(14), 2445–2466.

Bonannini, E., Cinotti, M., Puppio, M. L., & Sassu, M. (2017). Seismic response of a stock of social housings in Italy with R . C . and masonry materials . (Vol. 102, pp. 285–291). Advances in Engineering Research (AER), volume 102 285 Second International Conference on Mechanics, Materials and Structural Engineering (ICMMSE 2017).

Bosco, M., Ferrara, G. A. F., Ghersi, A., Marino, E. M., & Rossi, P. P. (2015). Predicting displacement demand of multi-storey asymmetric buildings by nonlinear static analysis and corrective eccentricities. *Engineering Structures*, *99*, 373–387.

Bosco, M., Ferrara, G. A. F., Ghersi, A., Marino, E. M., & Rossid, P. P. (2015). Seismic assessment of existing r.c. framed structures with in-plan irregularity by nonlinear static methods. *Earthquake and Structures*, *8*(2), 401–422.

Carley, K. M., Kamneva, N. Y., & Reminga, J. (2004). Response Surface Methodology 1 CASOS Technical Report, (October).

Çelebi, M., Bazzurro, P., Chiaraluce, L., Clemente, P., Decanini, L., Desortis, A., … Stephens, C. (2010). Recorded motions of the 6 April 2009 Mw 6.3 L'Aquila, Italy, earthquake and implications for building structural damage: Overview. *Earthquake Spectra*, *26*(3), 651–684.

CMIT. (2009). Circolare del Ministro delle Infrastrutture e dei Trasporti 2 febbraio 2009, n. 617, contenente le Istruzioni per l'applicazione delle "Nuove norme tecniche per le costruzioni" di cui al DM 14 gennaio 2008. Gazzetta Ufficiale della Repubblica Italiana n. 47 del 26 febbraio 2009, Supplemento Ordinario n. 27.

Consiglio Nazionale delle Ricerche. (2013). CNR-DT 212/2013. Istruzioni per la Valutazione Affidabilistica della Sicurezza Sismica di Edifici Esistenti.

De Stefano, M., & Pintucchi, B. (2002). A model for analyzing inelastic seismic response of plan-irregular building structures. In *15th ASCE Engineering Mechanics Conference*. New York.

De Stefano, M., & Pintuchi, B. (2010). Predicting torsion-induced lateral displacements for pushover analysis: Influence of torsional system characteristics. *Earthquake Engineering and Structural Dynamics*, *39*(March), 1369–1394. https://doi.org/10.1002/eqe

De Stefano, M., Tanganelli, M., & Viti, S. (2014). Variability in concrete mechanical properties as a

source of in-plan irregularity for existing RC framed structures. *Engineering Structures*, *59*, 161–172.
EC8-1. (2004). Eurocode 8: Design of structures for earthquake resistance—Part 1: General rules, seismic actions and rules for buildings. Brussels: European Committee for Standardization.
EC8-3. (2005). Eurocode 8: Design of structures for earthquake resistance—Part 3: Assessment and retrofitting of buildings. Brussels: European Committee for Standardization.
EN 1998-1. (2004). EN 1998-1: Eurocode 8 - Design of structures for earthquake resistance. Part 1: General rules, seismic actions and rules for buildings. *CEN*, *1*, 1–229.
Fajfar, P. (2000). A Nonlinear Analysis Method for Performance-Based Seismic Design. *Earthquake Spectra*, *16*, 573–592. https://doi.org/10.1193/1.1586128
Fajfar, P., Marusic, D., & Perus, I. (2005). Torsional Effects in the Pushover-Based Seismic Analysis of Buildings. *Journal of Earthquake Engineering*, *9*(6), 831–854.
FEMA. (2006). Techniques for the Seismic Rehabilitation of Existing Buildings FEMA 547. *Federal Emergency Management Agency, Washington, D.C.*, 571.
Garcia, O., Islas, A., & Ayala, A. G. (2004). Effect of the In-Plan Distribution of Strength on the Non-Linear Seismic Response of Torsionally Coupled Buildings. *13th World Conference on Earthquake Engineering* , (1891), Paper No. 1891.
Grünthal, G. (1998). *European Macroseismic Scale 1998*. *European Center of Geodynamics and …* (Vol. 15). Retrieved from http://scholar.google.com/scholar?hl=en&btnG=Search&q=intitle:European+Macroseismic+Scale+1998#0
Humar, J. L., & Kumar, P. (1999). Effect of orthogonal inplane structural elements on inelastic torsional response. *Earthquake Engineering and Structural Dynamics*, *28*(10), 1071–1097.
Keskikuru, T., Kokotti, H., Lammi, S., & Kalliokoski, P. (2001). Effect of strength deterioration on inelastic seismic torsional behaviour of asymmetric RC buildings. *Building and Environment*, *36*(10), 1109–1118.
Lavan, O., & de Stefano, M. (2013). Seismic behaviour and design of irregular and complex civil structures. *Geotechnical, Geological and Earthquake Engineering*, *24*.
Manfredi, V., & Masi, A. (2011). Seismic assessment of existing rc buildings based on different hazard maps. *Bollettino Di Geofisica Teorica Ed Applicata*, *52*(2), 1–20. https://doi.org/10.1061/(ASCE)ST.1943-541X.209; (2008) Nuove Norme Tecniche Per Le Costruzioni NTC2008, , NTC2008 - Decreto Ministeriale D.M. G. U. n. 29, 04.02.2008 - Supplemento Ordinario n. 30 (in Italian); (2003) Primi Elementi In Materia Di Criteri Generali Per La Classificazione Sismica Del Territorio Nazionale E Di Normative Tecniche Per Le Costruzioni In Zona Sismica, , OPCM3274-Ordinanza del Presidente del Consiglio dei Ministri n.3274/2003, Supplemento ordinario G. U. n. 105, 8 maggio 2003 (in Italian
Maru, D., & Fajfar, P. (2005). On the inelastic seismic response of asymmetric buildings under bi-axial excitation. *Earthquake Engineering and Structural Dynamics*, *34*(8), 943–963.
Mittal, A. K., & Jain, A. K. (1995). Effective strength eccentricity concept for inelastic analysis of asymmetric structures. *Earthquake Engineering & Structural Dynamics*, *24*(1), 69–84.
Montgomery, C. (n.d.). Progettazione e analisi degli esperimenti, 1–18.
Muller, D., Forster, V., & Graunbner, C.-A. (2017). Influence of Material Spatial Variability on the Reliability of Masonry Walls in Compression. In *13th Canadian Masonry Symposium, At Halifax*.
Prestandard and Commentary for the Seismic Rehabilitation of Buildings - FEMA 356. (2000).
Puppio, M., Pellegrino, M., Giresini, L., & Sassu, M. (2017). Effect of Material Variability and Mechanical Eccentricity on the Seismic Vulnerability Assessment of Reinforced Concrete Buildings. *Buildings*, *7*(4), 66.
Sadek, A. W., & Tso, W. K. (1989). Strength eccentricity concept for inelastic analysis of asymmetrical structures. *Engineering Structures*, *11*(3), 189–194. https://doi.org/10.1016/0141-0296(89)90006-0
Sassu, M., Puppio, M. L., & Mannari, E. (2017). Seismic Reinforcement of a R.C. School Structure with Strength Irregularities throughout External Bracing Walls. *Buildings*, *7*(3), 58.
Shinozuka, M., Feng, M. Q., Lee, J., & Naganuma, T. (2000). Statistical Analysis of Fragility Curves.

Journal of Engineering Mechanics, *126*(12), 1224–1231.

Sudret, B., Mai, C., & Konakli, K. (2014). Assessment of the lognormality assumption of seismic fragility curves using non-parametric representations, (April), 1157–1174.

Tanganelli, M., Viti, S., De Stefano, M., & Reinhorn, A. M. (2013). Influence of Infill Panels on the Seismic Response of Existing RC Builidings: A Case Study. In O. Lavan & M. De Stefano (Eds.), *Seismic Behaviour and Design of Irregular and Complex Civili Structures*. Geotechnical, Geological and Earthquake Engineering.

Titi, A., Biondini, F., & Frangopol, D. M. (2016). Cost-based recovery processes and seismic resilience of aging bridges.

Varadharajan, S., Sehgal, V. K., & Saini, B. (2012). Review of different structural irregularities in buildings. *Journal of Structural Engineering (India)*, *39*(5), 538–563.

Vona, M. (2014). Fragility Curves of Existing RC Buildings Based on Specific Structural Performance Levels. *Open Journal of Civil Engineering*, *04*(02), 120–134.

(appendix A)

Sclerometric Data. The columns are identified by a label as shown in Fig. 13

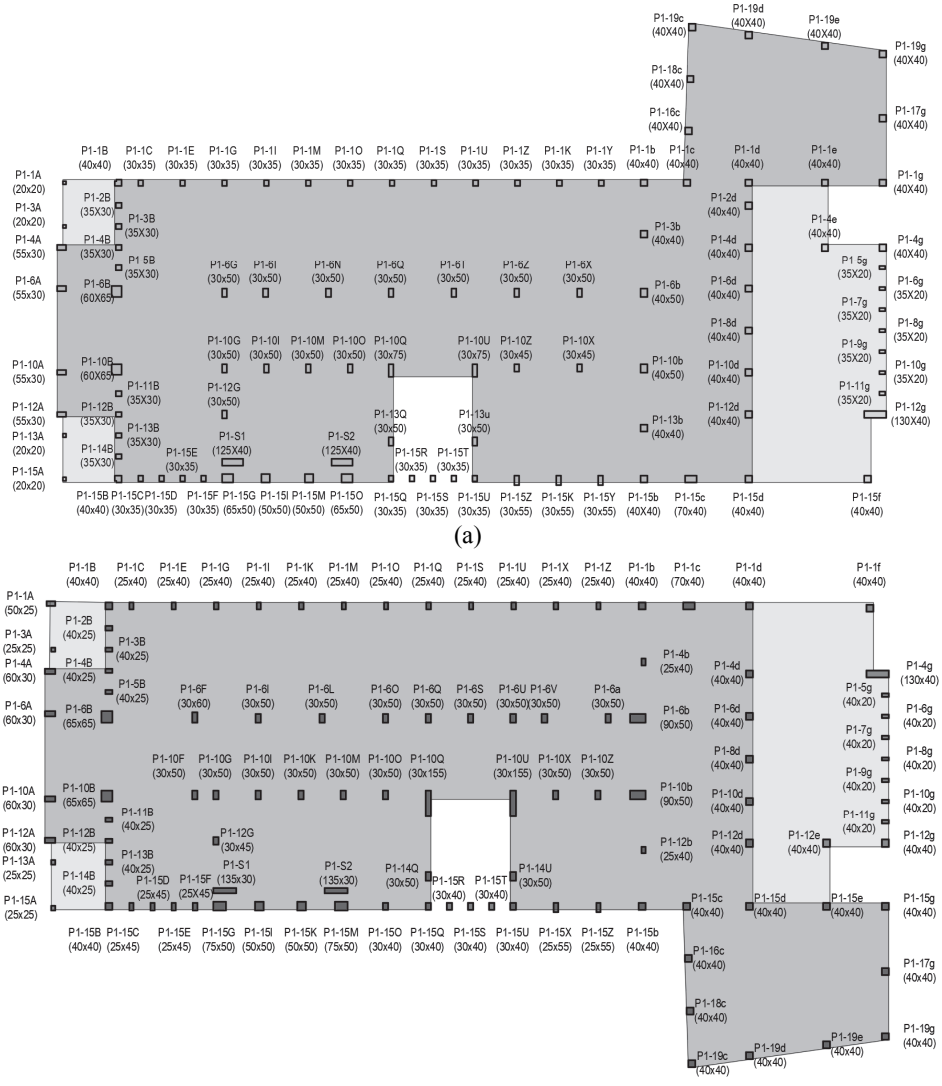

(a)

(b)

Fig. 13. Columns at the ground floor of the Building A (a) and C (b).

The hummer test is not done for the underground floor because of the lack accessibility of this level during the phase of survey.

Table A1. Sclerometric data.

N	Building A Ground floor			Building A First floor			Building A Second floor			Building C Ground floor			Building C First Floor			Building C Second floor		
	ID Column	$f_{c,i}$ [MPa]	$\Delta f_{c,i}$ [MPa]	ID Column	$f_{c,i}$ [MPa]	$\Delta f_{c,i}$ [MPa]	ID Column	$f_{c,i}$ [MPa]	$\Delta f_{c,i}$ [MPa]	ID Column	$f_{c,i}$ [MPa]	$\Delta f_{c,i}$ [MPa]	ID Column	$f_{c,i}$ [MPa]	$\Delta f_{c,i}$ [MPa]	ID Column	$f_{c,i}$ [MPa]	$\Delta f_{c,i}$ [MPa]
1	P1-1A	16.7	4.8	P2-4A	42.4	6.2	P3-4A	51.7	6.4	P1-1A	33.9	5.9	P2-4A	33.5	5.9	P3-4A	35.8	6.0
2	P1-3A	22.8	5.3	P2-5A	38.0	6.1	P3-5A	43.9	6.2	P1-3A	34.2	5.9	P2-5A	29.1	5.7	P3-5A	41.5	6.2
3	P1-13A	15.5	4.7	P2-6A	17.0	4.9	P3-6A	45.0	6.3	P1-13A	29.1	5.7	P2-6A	45.0	6.3	P3-6A	44.0	6.2
4	P1-15A	44.0	6.2	P2-7A	39.4	6.1	P3-7A	37.7	6.1	P1-15A	29.7	5.7	P2-7A	51.8	6.4	P3-7A	37.4	6.0
5	P1-4e	37.3	6.0	P2-8A	35.6	6.0	P3-8A	34.3	5.9	P1-1f	19.0	5.0	P2-8A	50.6	6.4	P3-8A	35.4	6.0
6	P1-15f	37.3	6.0	P2-9A	40.9	6.1	P3-9A	35.7	6.0	P1-4g	33.8	5.9	P2-9A	47.3	6.3	P3-9A	34.9	6.0
7	P1-4g	46.3	6.3	P2-10A	33.2	5.9	P3-10A	47.7	6.3	P1-5g	38.1	6.1	P2-10A	32.1	5.9	P3-10A	40.1	6.1
8	P1-5g	38.4	6.1	P2-11A	24.3	5.4	P3-11A	36.7	6.0	P1-6g	43.9	6.2	P2-11A	35.3	6.0	P3-11A	34.4	5.9
9	P1-6g	31.8	5.8	P2-12A	31.1	5.8	P3-12A	41.2	6.2	P1-7g	28.8	5.7	P2-12A	33.7	5.9	P3-12A	36.1	6.0
10	P1-7g	49.3	6.4	P2-1B	37.3	6.0	P3-1B	37.3	6.0	P1-8g	23.2	5.4	P2-1B	38.2	6.1	P3-1B	38.2	6.1
11	P1-8g	26.4	5.6	P2-2B	25.4	5.5	P3-2B	42.7	6.2	P1-9g	22.1	5.3	P2-2B	38.2	6.1	P3-2B	39.7	6.1
12	P1-9g	36.0	6.0	P2-3B	19.9	5.1	P3-3B	42.8	6.2	P1-10g	21.5	5.2	P2-3B	42.4	6.2	P3-3B	44.4	6.2
13	P1-10g	40.6	6.1	P2-4B	30.1	5.8	P3-4B	29.2	5.7	P1-11g	26.6	5.6	P2-4B	51.6	6.4	P3-4B	36.8	6.0
14	P1-11g	15.3	4.7	P2-6B	37.3	6.0	P3-6B	33.4	5.9	P1-12g	34.3	5.9	P2-6B	42.3	6.2	P3-6B	33.8	5.9
15	P1-12g	40.6	6.1	P2-12B	37.3	6.0	P3-12B	43.3	6.2	P1-12e	38.2	6.1	P2-12B	47.4	6.3	P3-12B	38.2	6.1
16	P1-4A	22.6	5.3	P2-13B	37.3	6.0	P3-13B	37.3	6.0	P1-4A	26.9	5.6	P2-13B	38.2	6.1	P3-13B	38.2	6.1
17	P1-6A	27.3	5.6	P2-14B	37.3	6.0	P3-14B	37.3	6.0	P1-6A	28.7	5.7	P2-14B	38.2	6.1	P3-14B	38.2	6.1
18	P1-10A	37.0	6.0	P2-15B	37.3	6.0	P3-15B	37.3	6.0	P1-10A	26.8	5.6	P2-15B	38.2	6.1	P3-15B	38.2	6.1
19	P1-12A	38.0	6.1	P2-1C	27.2	5.6	P3-1C	30.2	5.8	P1-12A	35.2	6.0	P2-1C	38.2	6.1	P3-1C	47.3	6.3
20	P1-1B	29.7	5.7	P2-1D	40.6	6.1	P3-1D	41.4	6.2	P1-1B	50.2	6.4	P2-1D	42.4	6.2	P3-1D	29.3	5.7
21	P1-2B	35.3	6.0	P2-1E	26.0	5.5	P3-1E	49.7	6.4	P1-2B	51.4	6.4	P2-1E	41.2	6.2	P3-1E	39.9	6.1
22	P1-3B	54.3	6.5	P2-1F	27.7	5.6	P3-1F	57.9	6.7	P1-3B	32.7	5.9	P2-1F	40.2	6.1	P3-1F	36.5	6.0
23	P1-4B	44.8	6.3	P2-1G	32.7	5.9	P3-1G	35.2	6.0	P1-4B	33.3	5.9	P2-1G	37.8	6.1	P3-1G	32.3	5.9
24	P1-5B	29.6	5.7	P2-1H	33.1	5.9	P3-1H	56.0	6.6	P1-5B	27.1	5.6	P2-1H	43.2	6.2	P3-1H	44.4	6.2
25	P1-6B	38.9	6.1	P2-1I	30.7	5.8	P3-1I	46.1	6.3	P1-6B	31.7	5.8	P2-1I	42.4	6.2	P3-1I	43.1	6.2
26	P1-10B	50.2	6.4	P2-1L	27.6	5.6	P3-1L	38.4	6.1	P1-10B	39.6	6.1	P2-1J	41.2	6.2	P3-1J	53.3	6.5
27	P1-11B	44.0	6.2	P2-1M	23.5	5.4	P3-1M	35.5	6.0	P1-11B	40.6	6.1	P2-1K	41.2	6.2	P3-1K	54.0	6.5
28	P1-12B	56.0	6.6	P2-1N	37.3	6.0	P3-1N	46.1	6.3	P1-12B	33.3	5.9	P2-1L	36.4	6.0	P3-1L	51.8	6.4
29	P1-13B	57.9	6.7	P2-1O	37.3	6.0	P3-1O	39.0	6.1	P1-13B	29.7	5.7	P2-1M	52.1	6.5	P3-1M	49.6	6.4
30	P1-14B	53.6	6.5	P2-1P	37.3	6.0	P3-1P	37.3	6.0	P1-14B	48.6	6.4	P2-1N	45.8	6.3	P3-1N	52.4	6.5
31	P1-15B	53.1	6.5	P2-1Q	37.3	6.0	P3-1Q	37.3	6.0	P1-15B	42.0	6.2	P2-1O	37.6	6.1	P3-1O	43.7	6.2
32	P1-1C	25.9	5.5	P2-1R	37.3	6.0	P3-1R	37.3	6.0	P1-1C	34.6	6.0	P2-1P	30.2	5.8	P3-1P	44.6	6.2
33	P1-1E	31.9	5.8	P2-1S	37.3	6.0	P3-1S	37.3	6.0	P1-1E	39.8	6.1	P2-1Q	33.0	5.9	P3-1Q	30.4	5.8
34	P1-1G	31.1	5.8	P2-1T	37.3	6.0	P3-1T	37.3	6.0	P1-1G	38.2	6.1	P2-1R	25.6	5.5	P3-1R	44.6	6.2
35	P1-1I	25.7	5.5	P2-1U	37.3	6.0	P3-1U	37.3	6.0	P1-1I	37.3	6.0	P2-1S	33.9	5.9	P3-1S	41.8	6.2
36	P1-1M	45.6	6.3	P2-1V	37.3	6.0	P3-1V	37.3	6.0	P1-1K	44.4	6.2	P2-1T	36.7	6.0	P3-1T	45.8	6.3
37	P1-1O	37.3	6.0	P2-1Z	47.0	6.3	P3-1Z	46.2	6.3	P1-1M	46.5	6.3	P2-1U	44.7	6.3	P3-1U	34.8	6.0
38	P1-1Q	37.3	6.0	P2-1W	38.2	6.1	P3-1W	41.2	6.2	P1-1O	41.6	6.2	P2-1V	33.9	5.9	P3-1V	49.9	6.4
39	P1-1S	33.9	5.9	P2-1K	36.3	6.0	P3-1K	34.2	5.9	P1-1Q	34.1	5.9	P2-1X	38.1	6.1	P3-1X	46.6	6.3
40	P1-1U	32.6	5.9	P2-1X	49.4	6.4	P3-1X	38.7	6.1	P1-1S	33.9	5.9	P2-1Y	42.0	6.2	P3-1Y	46.5	6.3
41	P1-1Z	43.9	6.2	P2-1Y	51.4	6.4	P3-1Y	44.8	6.3	P1-1U	37.8	6.1	P2-1Z	37.4	6.0	P3-1Z	45.2	6.3
42	P1-1K	27.7	5.6	P2-1a	40.3	6.1	P3-1a	47.4	6.3	P1-1X	36.6	6.0	P2-1a	47.9	6.3	P3-1a	37.8	6.1
43	P1-1Y	27.2	5.6	P2-1b	33.1	5.9	P3-1b	41.5	6.2	P1-1Z	40.9	6.1	P2-6F	38.2	6.1	P3-6F	30.4	5.8
44	P1-6G	55.8	6.6	P2-3b	37.3	6.0	P3-6G	37.3	6.0	P1-6F	47.6	6.3	P2-6I	45.3	6.3	P3-6I	38.7	6.1
45	P1-6I	27.9	5.7	P2-6G	22.4	5.3	P3-6I	37.3	6.0	P1-6I	53.1	6.5	P2-6L	46.8	6.3	P3-6L	48.0	6.3
46	P1-6N	30.4	5.8	P2-6I	37.3	6.0	P3-6Q	37.3	6.0	P1-6L	50.7	6.4	P2-6O	48.1	6.3	P3-6O	43.7	6.2
47	P1-6Q	20.1	5.1	P2-6N	37.3	6.0	P3-6T	37.3	6.0	P1-6O	52.3	6.5	P2-6Q	48.3	6.3	P3-6Q	38.1	6.1
48	P1-6T	12.7	4.4	P2-6Q	37.3	6.0	P3-6Z	37.3	6.0	P1-6Q	45.9	6.3	P2-6S	50.6	6.4	P3-6S	38.2	6.1
49	P1-6Z	20.8	5.2	P2-6T	37.3	6.0	P3-6X	36.7	6.0	P1-6S	50.1	6.4	P2-6U	44.6	6.2	P3-6U	52.1	6.5
50	P1-6X	37.3	6.0	P2-6Z	37.3	6.0	P3-6b	30.3	5.8	P1-6U	51.8	6.4	P2-6V	40.7	6.1	P3-6V	34.9	6.0
51	P1-10G	29.4	5.7	P2-6X	28.2	5.7	P3-10G	48.6	6.4	P1-6V	42.4	6.2	P2-6a	40.9	6.1	P3-6a	35.1	6.0
52	P1-10I	37.5	6.0	P2-6b	39.0	6.1	P3-10I	40.6	6.1	P1-6a	34.2	5.9	P2-10F	46.2	6.3	P3-10F	35.0	6.0
53	P1-10M	40.6	6.1	P2-10G	39.3	6.1	P3-10O	29.7	5.7	P1-10F	26.9	5.6	P2-10G	42.9	6.2	P3-10G	40.7	6.1
54	P1-10O	38.1	6.1	P2-10I	29.9	5.8	P3-10Q	29.0	5.7	P1-10G	35.1	6.0	P2-10I	45.6	6.3	P3-10I	41.0	6.2
55	P1-10Q	24.3	5.4	P2-10O	43.3	6.2	P3-10U	30.9	5.8	P1-10I	25.2	5.5	P2-10O	42.3	6.2	P3-10O	39.1	6.1
56	P1-10U	24.1	5.4	P2-10Q	38.7	6.1	P3-10Z	27.4	5.6	P1-10K	25.5	5.5	P2-10Q	37.6	6.1	P3-10Q	50.1	6.4
57	P1-10Z	29.6	5.7	P2-10U	55.0	6.6	P3-10X	42.8	6.2	P1-10M	22.8	5.3	P2-10U	30.9	5.8	P3-10U	34.8	6.0
58	P1-10X	30.5	5.8	P2-10Z	37.3	6.0	P3-10b	31.4	5.8	P1-10O	37.2	6.0	P2-10X	41.6	6.2	P3-10X	50.1	6.4
59	P1-12G	29.3	5.7	P2-10X	49.1	6.4	P3-15C	37.3	6.0	P1-10Q	34.8	6.0	P2-10Z	43.1	6.2	P3-10Z	45.2	6.3
60	P1-15C	36.3	6.0	P2-10b	46.4	6.3	P3-15D	37.3	6.0	P1-10U	30.4	5.8	P2-12G	48.6	6.4	P3-15C	38.2	6.1
61	P1-15D	50.3	6.4	P2-12G	37.3	6.0	P3-15E	37.3	6.0	P1-10X	53.7	6.5	P2-14G	49.1	6.4	P3-15D	43.1	6.2
62	P1-15E	59.7	6.7	P2-13b	37.3	6.0	P3-15F	37.3	6.0	P1-10Z	51.9	6.4	P2-15C	38.2	6.1	P3-15E	28.7	5.7
63	P1-15F	50.7	6.4	P2-15C	37.3	6.0	P3-15G	31.8	5.8	P1-12G	38.4	6.1	P2-15D	35.7	6.0	P3-15F	32.8	5.9
64	P1-15G	40.9	6.1	P2-15D	37.3	6.0	P3-15I	32.2	5.9	P1-15C	26.8	5.6	P2-15E	38.2	6.1	P3-15G	31.4	5.8
65	P1-15I	41.0	6.2	P2-15E	37.3	6.0	P3-15M	49.4	6.4	P1-15D	31.2	5.8	P2-15F	33.4	5.9	P3-15I	51.4	6.4
66	P1-15M	46.9	6.3	P2-15F	37.3	6.0	P3-15O	36.4	6.0	P1-15E	29.8	5.8	P2-15G	41.3	6.2	P3-15K	34.0	5.9
67	P1-15O	43.1	6.2	P2-15G	31.8	5.8	P3-15Q	37.3	6.0	P1-15F	25.2	5.5	P2-15I	51.4	6.4	P3-15M	36.7	6.0

N	Building A Ground floor			Building A First floor			Building A Second floor			Building C Ground floor			Building C First Floor			Building C Second floor		
	ID Column	$f_{c,i}$ [MPa]	$\Delta f_{c,i}$ [MPa]	ID Column	$f_{c,i}$ [MPa]	$\Delta f_{c,i}$ [MPa]	ID Column	$f_{c,i}$ [MPa]	$\Delta f_{c,i}$ [MPa]	ID Column	$f_{c,i}$ [MPa]	$\Delta f_{c,i}$ [MPa]	ID Column	$f_{c,i}$ [MPa]	$\Delta f_{c,i}$ [MPa]	ID Column	$f_{c,i}$ [MPa]	$\Delta f_{c,i}$ [MPa]
68	P1-15Q	37.3	6.0	P2-15I	32.2	5.9	P3-15R	37.3	6.0	P1-15G	35.8	6.0	P2-15K	34.0	5.9	P3-15O	34.8	6.0
69	P1-15R	37.3	6.0	P2-15M	49.4	6.4	P3-15S	37.3	6.0	P1-15I	30.6	5.8	P2-15M	36.7	6.0	P3-15Q	35.1	6.0
70	P1-15S	38.1	6.1	P2-15O	47.3	6.3	P3-15T	37.3	6.0	P1-15K	30.7	5.8	P2-15O	34.8	6.0	P3-15R	32.5	5.9
71	P1-15T	37.3	6.0	P2-15Q	37.3	6.0	P3-15U	37.3	6.0	P1-15M	35.2	6.0	P2-15Q	35.1	6.0	P3-15S	46.8	6.3
72	P1-15U	46.7	6.3	P2-15R	37.3	6.0	P3-15V	37.3	6.0	P1-15O	31.8	5.8	P2-15R	32.5	5.9	P3-15T	39.5	6.1
73	P1-15Z	39.2	6.1	P2-15S	37.3	6.0	P3-15Z	21.9	5.3	P1-15Q	22.7	5.3	P2-15S	46.8	6.3	P3-15U	37.6	6.1
74	P1-15K	40.4	6.1	P2-15T	37.3	6.0	P3-15W	35.5	6.0	P1-15R	27.7	5.6	P2-15T	39.5	6.1	P3-15V	35.7	6.0
75	P1-15Y	32.4	5.9	P2-15U	37.3	6.0	P3-15K	52.0	6.5	P1-15S	25.5	5.5	P2-15U	37.6	6.1	P3-15X	47.3	6.3
76	P1-1b	39.0	6.1	P2-15V	37.3	6.0	P3-15X	37.4	6.0	P1-15T	27.8	5.7	P2-15V	36.4	6.0	P3-15Y	49.3	6.4
77	P1-3b	48.9	6.4	P2-15Z	33.6	5.9	P3-15Y	31.5	5.8	P1-15U	30.6	5.8	P2-15X	44.0	6.2	P3-15Z	52.1	6.5
78	P1-6b	39.1	6.1	P2-15W	37.2	6.0	P3-15a	43.3	6.2	P1-15X	35.5	6.0	P2-15Y	46.1	6.3	P3-15a	23.6	5.4
79	P1-10b	32.8	5.9	P2-15K	43.2	6.2	P3-15b	31.2	5.8	P1-15Z	28.3	5.7	P2-15Z	34.9	6.0	P3-1b	43.9	6.2
80	P1-13b	37.9	6.1	P2-15X	40.4	6.1	P3-1d	37.3	6.0	P1-1b	30.9	5.8	P2-15a	38.9	6.1	P3-4b	38.2	6.1
81	P1-15b	37.3	6.0	P2-15Y	36.4	6.0	P3-2d	37.5	6.0	P1-4b	33.4	5.9	P2-1b	39.7	6.1	P3-6b	38.2	6.1
82	P1-1d	37.3	6.0	P2-15a	30.9	5.8	P3-3d	42.0	6.2	P1-6b	41.6	6.2	P2-4b	38.2	6.1	P3-10b	38.2	6.1
83	P1-2d	37.3	6.0	P2-15b	28.4	5.7	P3-4d	41.8	6.2	P1-10b	28.0	5.7	P2-6b	36.0	6.0	P3-12b	38.2	6.1
84	P1-4d	37.3	6.0	P2-1d	37.3	6.0	P3-5d	39.5	6.1	P1-12b	27.4	5.6	P2-10b	37.8	6.1	P3-15b	39.0	6.1
85	P1-6d	28.4	5.7	P2-2d	40.1	6.1	P3-6d	40.2	6.1	P1-15b	25.1	5.5	P2-12b	45.8	6.3	P3-1d	38.2	6.1
86	P1-8d	39.6	6.1	P2-3d	56.0	6.6	P3-7d	35.5	6.0	P1-1d	32.2	5.9	P2-15b	45.1	6.3	P3-2d	54.5	6.5
87	P1-10d	37.3	6.0	P2-4d	51.6	6.4	P3-8d	43.5	6.2	P1-4d	19.1	5.1	P2-1d	38.2	6.1	P3-3d	55.4	6.6
88	P1-12d	37.3	6.0	P2-5d	33.3	5.9	P3-9d	40.9	6.1	P1-6d	33.9	5.9	P2-2d	28.0	5.7	P3-4d	47.6	6.3
89	P1-15d	41.7	6.2	P2-6d	41.0	6.2	P3-10d	28.3	5.7	P1-8d	21.2	5.2	P2-3d	38.9	6.1	P3-5d	46.5	6.3
90	P1-15c	34.9	6.0	P2-7d	39.7	6.1	P3-11d	36.6	6.0	P1-10d	30.0	5.8	P2-4d	41.9	6.2	P3-6d	55.9	6.6
91	P1-1e	37.3	6.0	P2-8d	31.5	5.8	P3-12d	32.3	5.9	P1-12d	35.4	6.0	P2-5d	40.2	6.1	P3-7d	49.6	6.4
92	P1-1c	23.1	5.4	P2-9d	47.5	6.3	P3-13d	37.5	6.0	P1-15c	18.1	5.0	P2-6d	42.3	6.2	P3-8d	50.9	6.4
93	P1-16c	37.3	6.0	P2-10d	35.5	6.0	P3-14d	42.2	6.2	P1-16c	15.0	4.6	P2-7d	45.6	6.3	P3-9d	50.6	6.4
94	P1-18c	37.3	6.0	P2-11d	39.1	6.1	P3-15d	37.3	6.0	P1-18c	22.0	5.3	P2-8d	28.8	5.7	P3-10d	29.8	5.8
95	P1-19c	37.3	6.0	P2-12d	36.4	6.0				P1-19c	16.4	4.8	P2-9d	37.0	6.0	P3-11d	34.6	6.0
96	P1-19d	37.3	6.0	P2-13d	39.0	6.1				P1-19d	22.1	5.3	P2-10d	45.1	6.3	P3-12d	35.2	6.0
97	P1-19e	37.3	6.0	P2-14d	40.9	6.1				P1-19e	19.8	5.1	P2-11d	42.9	6.2	P3-13d	30.6	5.8
98	P1-1g	37.3	6.0	P2-15d	37.3	6.0				P1-19g	38.2	6.1	P2-12d	29.5	5.7	P3-14d	36.7	6.0
99	P1-17g	37.3	6.0							P1-17g	38.2	6.1	P2-13d	44.9	6.3	P3-15d	38.2	6.1
100	P1-19g	37.3	6.0							P1-15g	38.2	6.1	P2-14d	47.3	6.3	P3-1c	38.2	6.1
101	P1-S1	31.0	5.8							P1-15e	20.3	5.2	P2-15d	38.2	6.1	P3-15c	38.2	6.1
102	P1-S2	33.4	5.9							P1-15d	19.9	5.1	P2-1c	38.2	6.1			
103										P1-1c	34.8	6.0	P2-15c	38.2	6.1			
104										P1-S1	41.2	6.2						
105										P2-S2	33.2	5.9						

The Label of Table are referred to a grid in x and y direction.
The letter “P” indicates Pillars, and is common to all the labels;
The number 1,2 and 3 indicates respectively the ground, the first and the second floor;
The number after the score is referred to the x grid;
The letter after the score is referred to the y grid;
The letter S after the score indicate squat elements.